CMLS, Cell. Mol. Life Sci. 62 (2005) 1724–1733
1420-682X/05/151724-10
DOI 10.1007/s00018-005-5141-0

CMLS Cellular and Molecular Life Sciences

Research Article

Aluminum-triggered structural modifications and aggregation of β-amyloids

F. Ricchelli [d], D. Drago [a], B. Filippi [b], G. Tognon [a] and P. Zatta [a, *]

[a] CNR Institute of Biomedical Technologies, Metalloproteins Unit, Department of Biology, University of Padova Viale G. Colombo 3-35121 Padova (Italy), Fax: +39 049 8276348, e-mail: zatta@mail.bio.unipd.it
[b] Department of Chemical Sciences, University of Padova, Padova (Italy)

Received 29 March 2005; received after revision 10 May 2005; accepted 25 May 2005
Online First 30 June 2005

Abstract. We investigated the structural effects induced by Al^{3+} on different β-amyloid (Aβ) fragments at pH 7.4 and T= 25 °C, with particular attention given to the sequences 1–40 and 1–42. Al^{3+} caused peptide enrichment in β sheet structure and formation of solvent-exposed hydrophobic clusters. These intermediates evolved to polymeric aggregates which organized in fibrillar forms in the case of the Al^{3+}-$A\beta_{(1-42)}$ complex. Comparative studies showed that Zn^{2+} and Cu^{2+} were much less efficient than Al^{3+} in stimulating the spontaneous aggregation/fibrillogenesis of Aβs. Studies with liposomes as membrane models showed dramatic changes in the structural properties of the lipid bilayer in the presence of Al^{3+}-Aβ complexes, suggesting a major role of Al^{3+} in Aβ-induced cell dysfunction. Al^{3+} effects were abolished by desferrioxamine mesylate (DFO) only in solution. We concluded that, in vivo, DFO may act as a protective agent by preventing or reverting Aβ aggregation in the extracellular spaces.

Key words. Alzheimer; metal ions; aluminum; amyloid; copper; zinc.

Alzheimer's disease (AD) is the most common cause of intellectual impairment in adults. It is characterized by progressive dementia, cortical neuronal loss, and the widespread appearance of neurofibrillary tangles (NFTs) in the cytoplasm of degenerating neurons, and senile plaques (SPs) in the extracellular liquid. The plaques are composed of β-structured fibrils made up of β-amyloid protein (Aβ), a family of peptides 39–43 amino acid residues long. Under conditions still not clearly known, Aβ aggregates and accumulates to form amyloid fibrils [1, 2]. The propensity to aggregation depends on the amino acid sequence. Among the most representative Aβ peptides in vivo, $A\beta_{(1-40)}$ is found as the predominant soluble species in biological fluids whereas $A\beta_{(1-42)}$ mainly contributes to plaque deposits.

Some authors believe that Aβ deposits are responsible for the progressive neurodegeneration during the disease [3, 4]. In vitro experiments suggest that the soluble Aβ monomers require conversion to a largely β-pleated sheet conformation and subsequent aggregation into a structural fibrillar form before they can confer neurotoxicity. However, there is presently a large consensus that small soluble Aβ oligomers, either in the form of protofibrils (PFs) or small 'diffusible' Aβ oligomers (ADDLs), could be the real toxic entities during the course of the amyloid polymerization process [5–8]. Other authors propose that both fibrillar and pre-fibrillar amyloid species induce in vitro neurotoxicity and cell death [9–11]. Since Aβ oligomerization seems to be initiated intracellularly [7, 12], soluble membrane diffusible Aβ species might constitute an early component of the neurodegenerative process, whereas extracellular insoluble polymeric entities might be responsible for late toxicity in AD [for a review see ref. 13].

Important chemical and biophysical factors (e.g., pH, free radicals, temperature, incubation time, peptide length and concentration, lipid, proteins, chemical chaperones) that

* Corresponding author.

might be involved in the aggregation and fibrillogenesis of Aβ have been extensively discussed in many studies [for a review see ref.14]. Among these etiopathogenic factors or cofactors hypothetically involved in AD, exposure to certain metal ions has been proposed as a relevant risk factor for developing the disease. In particular, complexation of metals might provide the stimulus required to overcome the thermodynamic barrier to autopolymerization of Aβ [15, 16]. This might explain the elevated concentrations of copper, zinc, iron, aluminum and other metals found colocalized with Aβ in senile plaques [17–20].

The influence of metal ions such as Fe^{3+}, Cu^{2+}, and Zn^{2+} in stimulating Aβ aggregation as well as their interaction modalities with the β peptide have been widely studied in vitro. Zn^{2+} appears to be very efficient in inducing fast precipitation of Aβs and formation of protease-resistant aggregates both at acidic and alkaline pH [15]. In contrast, Cu^{2+} and Fe^{3+} show limited propensity to aggregate at pH $\geq$ 7 whereas aggregation is drastically potentiated at slightly acidic pH [21–24].

Al^{3+} has long been recognized as a neurotoxic element in several biological models, but its etiological role in AD is still controversial [25, 26]. On the basis of a variety of physiopathological effects of Al^{3+} in cell cultures and experimental animals, and its consistent occurrence in NFTs [27] and SPs [28], aluminum has been proposed as a major risk factor in some categories of patients prone/sensitive to Al^{3+} intoxication with consequent occurrence of neurological dysfunctions. Al^{3+} has also been reported to influence the aggregation and toxicity of Aβ in vitro and in transgenic mice [21, 29–33]. Nevertheless, the interaction properties of Al^{3+} with β amyloids have so far received less attention than those of other biometals.

In this paper, we report a detailed characterization of the changes in conformational and aggregational properties of different amyloid sequences induced by Al^{3+}. We show that, at alkaline pH, Al^{3+} is a more efficient inducer of amyloid aggregation/fibrillogenesis than zinc or copper, can rapidly form fibrils even at micromolar concentrations and, in solution, its effects can be fully antagonized by the trivalent cation chelator desferrioxamine mesylate (DFO).

Materials and methods

Materials

β-Amyloids (fragments 1–16, 1–38, 1–40, 1–42; 95% pure by HPLC), thioflavin T (ThT), 8-anilinonaphthalene-1-sulfonic acid (ANS), $ZnCl_2$, $Al(C_3H_5O_3)_3$, $CuSO_4$, L-α-dimyristoylphosphoglycerocholine (DMPC), 1–6-diphenyl-1,3,5-hexatriene (DPH), and N-acetyltyrosinamide were purchased from Sigma-Aldrich (St. Louis, Mo.). DFO was a gift from Dr T. Kruck, University of Toronto, Canada.

$Al(C_3H_5O_3)_3$ was used instead of Al inorganic salts in order to improve the metal soluble concentrations [26]. The complex was purified and stored according to the protocol reported by Zatta et al. [34].

The levels of metal contamination in the buffers were assayed by atomic absorption spectroscopy. In all preparations, metal traces were below the detection limit.

All other chemicals were of the purest analytical grade.

All experiments were carried out in 0.1 M Tris/HCl buffer plus 150 mM NaCl (standard medium), at pH 7.4 and T = 25 °C.

Fluorescence measurements

Fluorescence measurements of the different β-Amyloids were recorded with a Perkin Elmer LS 50B spectrophotofluorimeter equipped with a thermostatic cell holder and magnetic stirring. For intrinsic fluorescence, tyrosine (Tyr) fluorescence was excited at 275 nm and collected in the range 290–350 nm. For extrinsic fluorescence, ANS binding to $A\beta_{(1-40)}$ and $A\beta_{(1-42)}$ was followed by the increase of fluorescence emission of ANS in the range 400–700 nm (λ_{exc} = 360 nm). The ratio between the dye concentration (25 µM) and the peptide in all experiments was kept equal to 5. ThT (12 µM) binding at different peptide concentrations ranging from 0.5 to 40 µM was followed by the increase of fluorescence intensity at 482 nm with excitation at 450 nm.

Circular dichroism measurements (CD)

Circular dichroism (CD) spectra were determined in the spectral range 260–195 nm at 25 °C using a Jasco Model J-715 automatic recording CD spectrophotometer. Fused quartz cells with a path length of 0.1 and 0.05 cm were used. Each spectrum, corrected for the blank baseline, was the average of eight scans. All the operations were performed using Jasco CD data manipulation J-715 software. The contribution to the peptide structure of the various components (α helix, β structure and random coil) was calculated after deconvolution of the CD spectra on the basis of Bohm's parameters [35].

Transmission electron microscopy measurements

Diluted aliquots of amyloid preparations were absorbed onto glow-discharged carbon-coated butwar films on 400-mesh copper grids. The grids were negatively stained with 1% uranyl acetate and observed at ×40,000 by transmission electron microscopy (TEM) (Hitachi H600).

Preparation of DPH-labeled liposomes

Small unilamellar vesicles of DMPC (mean external radius ~30 nm) were prepared by the ethanol injection method, as modified by Kremer et al. [36], by codissolving 15.3 µM DPH with 20.65 mM phospholipid in ethanol. The ethanolic solution (0.7 ml) was slowly injected into 10 ml of magnetically stirred standard medium at 35 °C, i.e.,

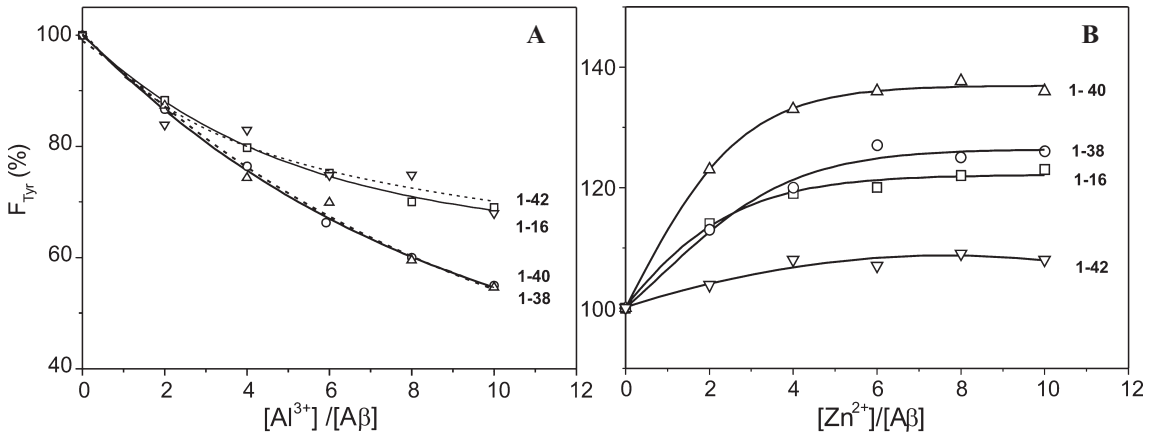

Figure 1. Al^{3+}- (*A*) and Zn^{2+}- (*B*) induced changes of the intrinsic fluorescence of β-amyloids (fragments 1–16, 1–38, 1–40, 1–42). Aβ concentrations were 5 µM in the standard medium (see Materials and methods). Tyr fluorescence was collected at 305 nm (λ excitation at 275 nm). The data are means of four determinations (SD±5%).

above the critical temperature (T_c) of the lipid phase transition. β-Amyloids and Aβ-Al^{3+} complexes were added to the liposomal dispersions after preparation. Excess Al^{3+} was removed from Aβ-Al^{3+} complexes before insertion into liposomes by 24-h dialysis against the standard medium (three buffer changes) in Spectra/Por Float-A-Lyzer tubes (cut-off = 1 kDa).

Results

This work illustrates the results of a comparative study of the β-amyloid aggregation due to Al^{3+}, Zn^{2+}, and Cu^{2+} under strictly comparable experimental conditions. Several papers have reported the effects of metal ions toward Aβ peptides at acidic pH and/or at 37 °C; such conditions dramatically accelerate the Aβ misfolding-aggregation process. We chose to perform our experiments at pH 7.4 and at T =25 °C; under these experimental conditions, the aggregation process is considerably delayed, thus allowing greater discrimination between the effects of the different metal ions.

Metal-induced conformational changes of β-amyloids as deduced by studies of intrinsic fluorescence

Figure 1 shows how increasing concentrations of Al^{3+} change the Tyr fluorescence of the various peptide sequences. The effects of Zn^{2+} are also reported. Al^{3+} quenched the peptide fluorescence emission, this effect being stronger in 1–38 and 1–40 peptides than in 1–16 and 1–42 (fig. 1A). In contrast, Zn^{2+} enhanced the Tyr fluorescence (fig. 1B), in agreement with previous results [37]. Experiments performed on N-acetyl-tyrosinamide dissolved in the same buffer showed that the fluorescence intensity of the free amino acid is not appreciably affected by the presence of the metals. These observations indicate that changes in the peptide fluorescence must be referred to as metal-promoted structural reorganization of the amyloid structure. Conversely, copper quenched the free tyrosine fluorescence to an extent comparable to that of amyloids (data not shown), most likely by a heavy atom/paramagnetic ion effect [38].

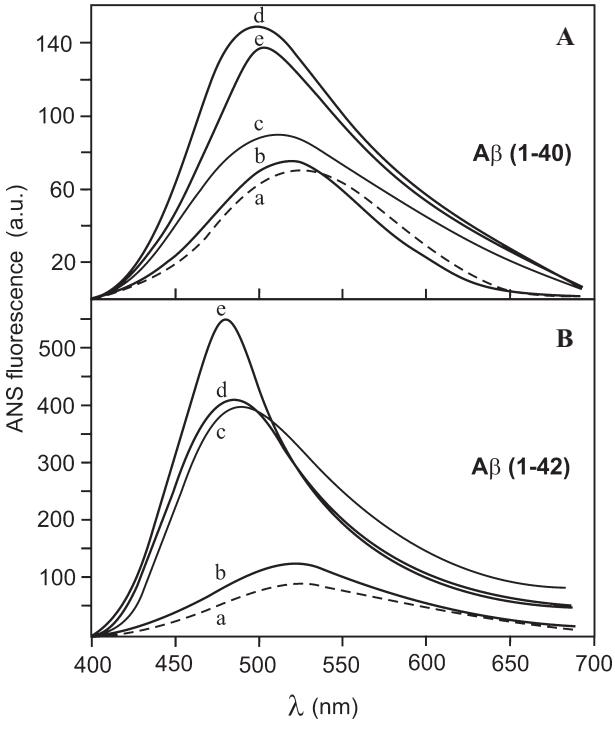

Figure 2. Fluorescence emission spectra of ANS before and after interaction with metal-free and metal-loaded $Aβ_{(1–40)}$ (*A*) and $Aβ_{(1–42)}$ (*B*) Trace a, ANS alone; trace b, ANS + Cu^{2+}-Aβ; trace c, ANS + Aβ; trace d, ANS + Zn^{2+}-Aβ; trace e, ANS + Al^{3+}-Aβ. Emission spectra were recorded from 400 to 700 nm with excitation at 360 nm. The [ANS]/[β-amyloid] ratio was equal to 5. Aβ was dissolved in the standard medium at 5 µM. The concentration of the different cations was 50 µM.

Surface hydrophobicity of β-amyloids as deduced by ANS fluorescence changes

Amyloids 1–40 and 1–42, which are the most representative Aβ peptides in vivo, were also tested for their surface hydrophobicity by following the fluorescence of ANS. According to Uversky et al. [39], changes in ANS fluorescence (enhancement of intensity and blue shift of the emission maximum) are characteristic hallmarks of the interaction of this dye with solvent-exposed hydrophobic clusters of partially folded peptides and proteins. Figure 2 shows that both Zn^{2+}- and Al^{3+}-containing β-amyloids increased the ANS fluorescence intensity and induced a blue shift of the emission λ_{max}, these effects being more pronounced in the 1–42 fragment (fig. 2B) compared to 1–40 (fig. 2A), especially in the presence of Al^{3+}. This means that native peptides are converted into partially folded conformations with solvent-exposed hydrophobic patches. Such conversion is not observed for the Cu^{2+}-Aβ complexes; rather, copper apparently inhibits the spontaneous increase of surface hydrophobicity in the 1–42 fragment. Partially folded intermediates should lead to an increased propensity to aggregate and/or form fibrils [39].

Changes of β-amyloid secondary structure as deduced by CD measurements

Aggregation and amyloid fibril formation are generally preceded by an increase of β structure in the peptide conformation [3]. CD experiments on freshly prepared metal-free peptides as well as Zn^{2+}- and Al^{3+}- amyloid (1–40 and 1–42) complexes revealed that both metals promote the formation of β sheet structure, with an increase of about 30% (in 1–40) and 40% (in 1–42) compared to the metal-free peptides (see table 1). In contrast, a preferential conversion to random coil structure in both peptides was noticed in the presence of Cu^{2+}.

Table 1. Secondary structure of $A\beta_{(1–40)}$ (20 µM) and $A\beta_{(1–42)}$ (10 µM) from CD spectra.

	Metal-free	+ Al^{3+}	+ Zn^{2+}	+ Cu^{2+}
$A\beta_{(1–40)}$				
α helix	9.0	6.7	7.1	10.0
β sheet	36.6	47.4	48.0	31.2
β turn	20.9	19.3	18.3	21.6
Random coil	35.6	31.3	32.9	39.5
$A\beta_{(1–42)}$				
α helix	10.2	8.0	7.7	10.9
β sheet	34.0	47.5	46.5	30.2
β turn	20.2	18.6	18.3	20.8
Random coil	36.4	31.2	33.1	39.6

Aggregation of β-amyloids as deduced by ThT fluorescence changes

ThT is known to rapidly associate with β-sheet-rich, aggregated forms of peptides giving rise to a new λ_{max} excitation at 450 nm and enhanced emission at 482 nm, as opposed to the 385 nm (ex) and 445 nm (em) of the free dye. This change is dependent on the aggregation state, as monomeric or dimeric peptides do not react with ThT [40]. We studied the effect of concentrations up to 40 µM (≤ 20 µM for Zn^{2+} due to precipitation) on the aggregational properties of the 1–40 and 1–42 peptides in the absence and presence of Zn^{2+}, Al^{3+}, and Cu^{2+} (fig. 3). ThT fluorescence was monitored within 10 min after preparation of the different samples. The most dramatic effects on the β-amyloid aggregational properties were obtained in the presence of Al^{3+}. ThT fluorescence already approached the maximal value at concentrations of Aβ as low as 2 µM in the 1–42 fragment, whereas higher concentrations of Aβ (~ 20 µM) were necessary for the 1–40 fragment to obtain similar effects. Conversely, Cu^{2+} did not appear to stimulate the Aβ spontaneous aggregation.

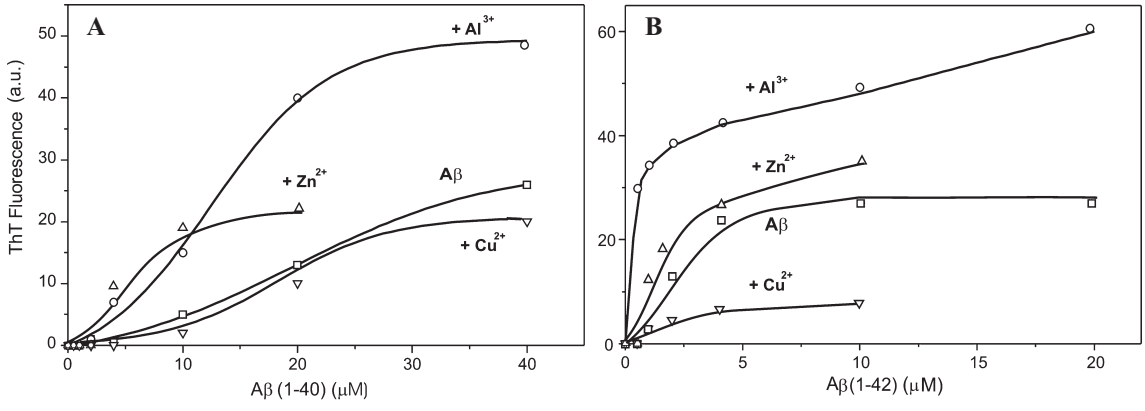

Figure 3. Fluorescence emission intensity of ThT as a function of metal-free and metal-loaded $A\beta_{(1–40)}$ (*A*) and $A\beta_{(1–42)}$ (*B*) concentrations. Metal concentration was 50 µM. ThT fluorescence at 482 nm (λ_{exc} = 450 nm) was collected immediately after addition of peptide aliquots to 15 µM ThT in the standard medium. The signal due to the free ThT was subtracted. Zn^{2+}- (and Cu^{2+} in $A\beta_{(1–42)}$) Aβs were followed for a narrower range of concentrations (<15 µM) due to precipitation. The data are means of three determinations (SD±10%).

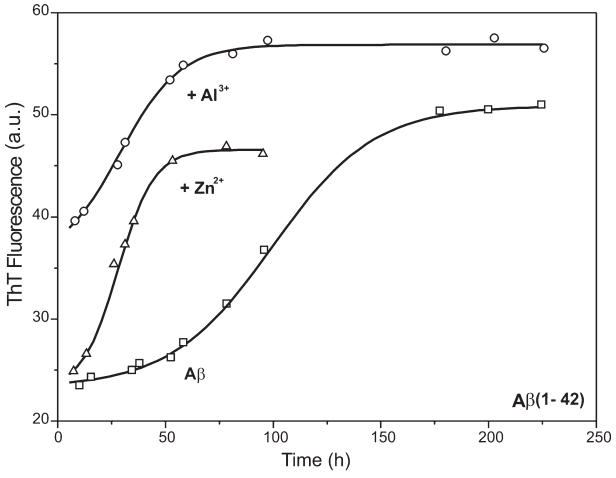

Figure 4. Kinetics of $A\beta_{(1–42)}$ aggregation in the absence and presence of Al^{3+} and Zn^{2+} as followed by the changes in ThT fluorescence emission intensity. Experimental conditions were as described in the legend to figure 3. $A\beta_{(1–42)}$ concentration was 5 µM. The data are means of three determinations (SD±8%).

Metal ions also affected the rate of aggregate formation, as shown in figure 4 where the kinetics of ThT fluorescence changes for 5 µM $A\beta_{(1–42)}$ in the absence and the presence of Zn^{2+} and Al^{3+} were followed over a period of 220 h (90 h for Zn^{2+}). In the presence of both Al^{3+} and Zn^{2+} the rate of aggregate formation was dramatically faster than in their absence, with Al^{3+} exhibiting the maximal stimulatory effect.

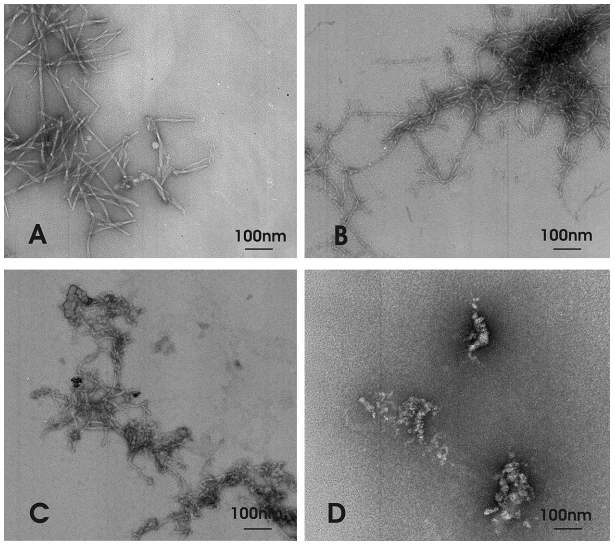

Figure 5. Electron micrographs of $A\beta_{(1–42)}$ in the absence (*A*) and presence (*B*) of Al^{3+}, Zn^{2+} (*C*) and Cu^{2+} (*D*). Al^{3+}-Aβ (2 µM), Zn^{2+}- and Cu^{2+}-Aβ (20 µM) complexes (metal concentration = 50 µM) and metal-free Aβ (20 µM) were left to incubate for 10 days in the standard medium at T= 25 °C.

Formation of fibrillar aggregates as deduced by electron microscopy experiments

Long-term incubations (>7 days depending on the amyloid concentration and the nature of the metal) lead to precipitation of metal-free and metal-containing amyloids. Electron microscopy studies of the precipitates after 10 days incubation show that Al^{3+} induced formation of fibrillar aggregates for $A\beta_{(1–42)}$ (fig. 5B). The fibrils could already be observed at very low peptide concentrations (2 µM). Under the same experimental conditions, much higher concentrations (20 µM) were necessary to induce spontaneous fibrillation (fig. 5A) whereas only small, amorphous structures were observed in the presence of 20 µM Cu^{2+}-Aβ (fig. 5D). In the micrographs of Zn^{2+}-$A\beta_{(1–42)}$ (20 µM), fibrillar forms shorter than those observed for Al^{3+}- $A\beta_{(1–42)}$ could be seen (fig. 5C). Extensive fibrillation of the Zn^{2+} complex, however, could be achieved under more drastic conditions (longer incubation periods, higher temperatures and peptide concentrations). In this case, the mature fibrils were structurally similar to those induced by Al^{3+}.

All $A\beta_{(1–40)}$ peptides, in the same time intervals and at up to 20 µM, formed mainly amorphous agglomerates (not shown).

Effects of metal-chelating agents on the conformational and aggregational properties of Al^{3+}-amyloid complexes

We investigated the effect of the trivalent ion chelator DFO on the changes in the conformational and aggregational properties of $A\beta_{(1–40)}$ and $A\beta_{(1–42)}$ induced by Al^{3+}. Figure 6 shows that the addition of Al^{3+} to $A\beta_{(1–42)}$ caused quenching of the intrinsic fluorescence (trace a), as also

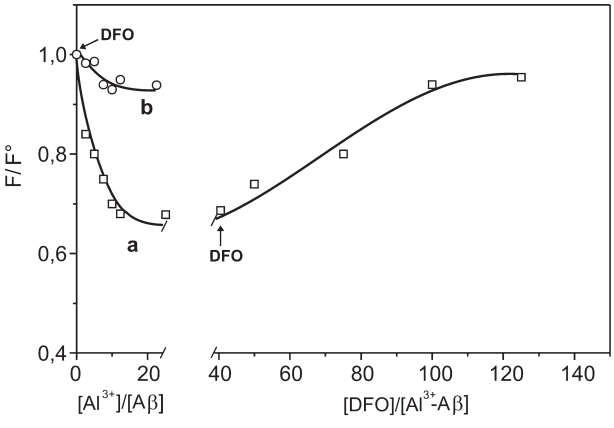

Figure 6. DFO antagonizing effect on the Al^{3+}-induced changes of the intrinsic fluorescence of $A\beta_{(1–42)}$. Aβ concentration was 5 µM. Tyr fluorescence was collected at 305 nm (λ excitation at 275 nm). The data are reported as the ratio between the fluorescence intensities (F) after addition of metal or DFO and the initial value in the absence of metal (F°). In trace a, increasing aliquots of DFO were added after the formation of the Al^{3+}-Aβ complex; in trace b, DFO (0.5 mM) was present before the addition of the metal.

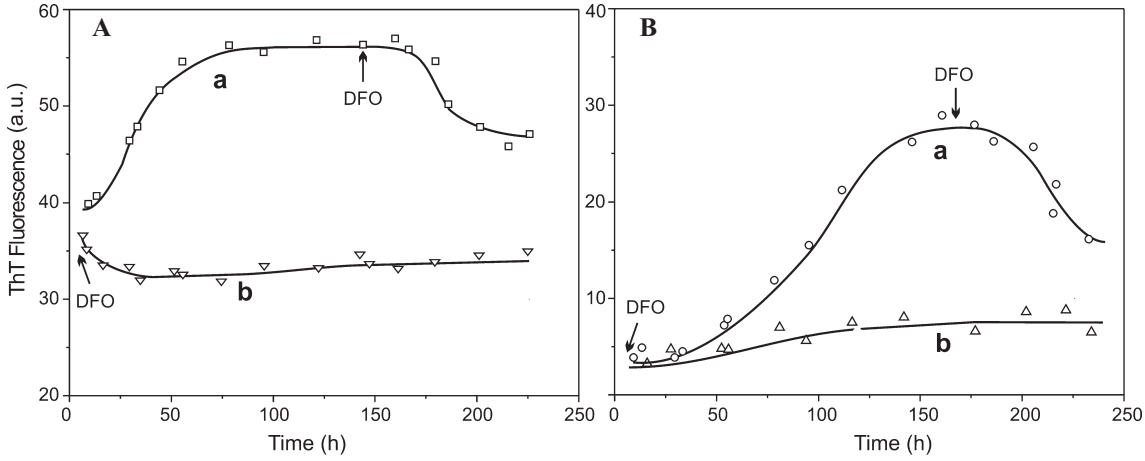

Figure 7. DFO antagonizing effect on the Al^{3+}-induced aggregation of $A\beta_{(1–42)}$ (A) and $A\beta_{(1–40)}$ (B) as deduced by ThT fluorescence changes. In trace a, DFO (0.5 mM) was added after formation of $A\beta_{(1–42)}$ aggregates; in trace b, DFO was present at the beginning of the experiment. $A\beta$ concentration was 5 µM. ThT fluorescence was collected at 482 nm (λ_{exc} = 450 nm).

reported in figure 1. Tyr fluorescence intensity was restored to the initial value when DFO was added after formation of the Al^{3+}-$A\beta$ complex. The Al^{3+}-induced fluorescence quenching could also be prevented by carrying out metal titration in the presence of DFO (trace b). Similar results were obtained in the case of $A\beta_{(1–40)}$. In conclusion, DFO was able to both inhibit and reverse the conformational changes promoted by Al^{3+} on the β-amyloid fragments.

Likewise, we studied the influence of DFO on the Al^{3+}-stimulated formation of $A\beta_{(1–42)}$ (fig. 7A) and $A\beta_{(1–40)}$ (fig. 7B) aggregates as indicated by the changes in ThT fluorescence. DFO was added both at the late (traces a) and early (trace b) stages of the aggregation process. The results indicate that DFO was able in both cases to counteract, albeit slowly, the metal-promoted aggregation. Electron microscopy experiments on the DFO-treated $A\beta$s showed that fibril formation was inhibited under these experimental conditions (data not shown).

Similar experiments carried out on the Zn^{2+}-$A\beta$ complexes revealed that DFO, in this case, antagonized the effect of the metal only marginally (data not shown).

Interaction of β-amyloids with lipid membranes

We also investigated whether Al^{3+}, which appears to be endowed with the highest aggregating potential among the metals examined, could be a biological factor capable of modulating the interaction of β-amyloids with the membranes. Soluble forms of $A\beta$ have been established to intercalate into the plasma membranes of neurons, directly disrupting various membrane activities and inducing neuronal cell death, their destabilizing properties being specific to the peptide conformation [41–44].

We studied the interaction of increasing concentrations of the most pathogenic $A\beta$ peptide, $A\beta_{(1–42)}$, both in its metal-free and Al^{3+}-complexed form, with DPH-labeled liposomes of DMPC as membrane models. Since Al^{3+} is able to alter per se the membrane structure [45], unbound metal was previously removed by dialysis (see Material and methods). To ensure comparable experimental conditions, metal-free $A\beta$ was also dialyzed for the same period of time.

We measured the $A\beta$-induced changes in the DPH fluorescence anisotropy which senses the structural architecture of the most hydrophobic domains of the lipid bilayer [46]. The measurements were performed in the temperature range 10–43 °C in order to explore the lipid phase transition from the gel (solid) to the liquid-crystalline (fluid) state (critical T of the transition, T_c, ~20 °C) (fig. 8). At all concentrations examined, metal-free $A\beta$ did not discernibly shift T_c as reported in figure 8 (for 6 µM $A\beta$) and

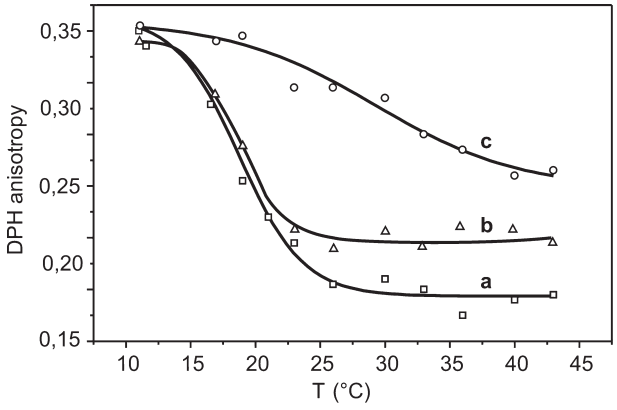

Figure 8. Temperature dependence of the anisotropy of DPH-labeled DMPC liposomes. DPH anisotropy was collected at 520 nm (λ_{exc} = 340 nm) in the absence of $A\beta$ (trace a), in the presence of 6 µM $A\beta_{(1–42)}$ (trace b), and in the presence of 6 µM Al^{3+}-$A\beta$ complex (trace c) after removal of unbound metal. The final phospholipid and dye concentrations were 1.58 mM and 1 µM, respectively. DMPC liposomes were prepared in the standard medium.

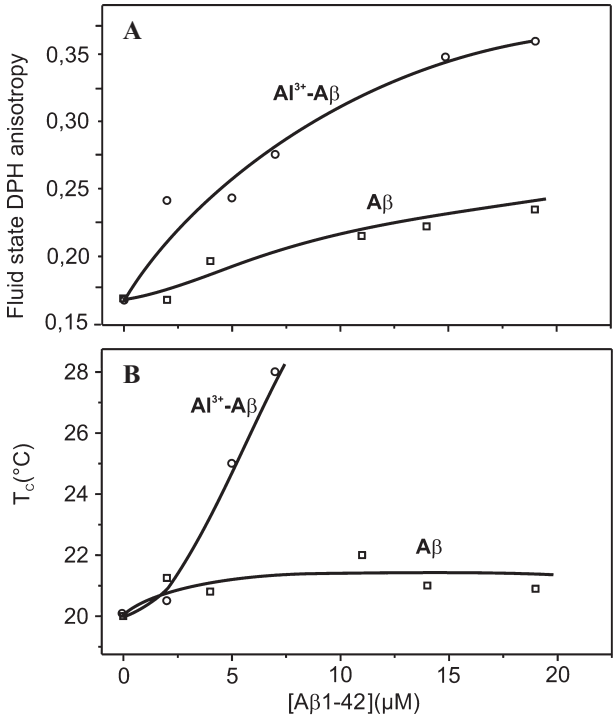

Figure 9. Anisotropy of DPH-labeled DMPC liposomes in the fluid state (*A*) and critical temperature of the lipid phase transition (*B*). DMPC liposomes were loaded with different concentrations of metal-free and Al^{3+}-bound $A\beta_{(1–42)}$. Experimental conditions were as described in the legend to figure 8.

figure 9A (for Aβ concentrations up to 20 μM), whereas DPH anisotropy increased considerably in the liquid-crystalline phase but not in the gel phase (figs 8, 9B). On the other hand, insertion of increasing concentrations (up to 20 μM) of the Al^{3+}-Aβ complex in DMPC liposomes dramatically increased the DPH anisotropy in the fluid state and shifted the T_c to higher T (see figs 8, 9A, B) until the lipid transition phase was completely abolished (above 12 μM). DFO added to the Aβ-membrane systems was unable to reverse the observed membrane structural alterations, even at low Al^{3+}-Aβ concentrations (not shown).

Discussion

Great interest in the effects of metal ions on β peptide misfolding and aggregation has been raised by the observation that high concentrations of metal ions are colocalized in the core of Alzheimer's amyloid plaques. Some metals have been shown to accelerate protein aggregation, stabilize amyloid fibrils, and increase the neurotoxic effects of Aβ peptides in vitro (see the introduction). These considerations would suggest that similar effects might be produced in vivo, thus stimulating studies on the interaction of different metal ions with Aβ peptides and on metal chelation as potential pharmacological treatment of AD [47–49].

In contrast to other biometals, the role of Al^{3+} in the pathogenesis of AD is still debated. Since there exists extensive literature demonstrating the neurotoxic effects of Al^{3+} in several biological models and its interference with a variety of cellular and metabolic processes, the involvement of Al^{3+} in AD should not be discarded. As has recently been proposed, Al^{3+} may not initiate AD but at the very least it may exacerbate the progression of the neurodegenerative process [26].

On this basis, our study focused on a detailed characterization of the conformational and aggregational changes stimulated by Al^{3+} on different Aβ fragments, in particular the most representative peptides in vivo, which correspond to the sequences $A\beta_{(1–40)}$ and $A\beta_{(1–42)}$. A comparison was made with the effects produced by other metal ions, namely Zn^{2+} and Cu^{2+}, under the same experimental conditions.

Our studies show clearly that Al^{3+} and, less markedly, Zn^{2+} are able to stimulate with great efficiency the aggregation of $A\beta_{(1–40)}/_{(1–42)}$ at alkaline pH. Aggregation is the ultimate result of a sequence of structural events that have been postulated to characterize the formation of misfolded protein aggregates, typically present in the various forms of the so-called 'conformational diseases' including AD [50]. Thus, binding of the metal shifts the peptide conformation, initially rich in random coil structure, to a β sheet structure (table 1) which favors the formation of partially folded intermediates characterized by exposure of hydrophobic clusters (fig. 2). These intermediates evolve to polymeric aggregates at a rate which is dramatically increased in the presence of Al^{3+} (figs 3, 4). In a relatively short period of time (10 days), the Al^{3+}-$A\beta_{(1–42)}$ aggregates are organized into well-structured fibrillar forms already at very low peptide concentrations (2 μM, fig. 5B). In contrast, fibril maturation is observed with lower rates and at higher peptide concentrations (20 μM) after spontaneous Aβ polymerization (fig.5A) and in the case of Zn^{2+}-$A\beta_{(1–42)}$ (fig. 5C). Our findings confirm previous studies on the effects of Zn^{2+} and Al^{3+} on Aβ aggregation (see the introduction). In addition, they state precisely that the relative potency of Al^{3+} is to markedly enhance the propensity of the peptide to give structured aggregates in terms of the rate of the process and peptide concentration required. From a practical point of view, this observation might be of paramount importance in those individuals sensitive to aluminum accumulation in terms of exposure due to professional occupation or as a consequence of pharmacological treatment [51].

Under our experimental conditions, Cu^{2+} did not catalyze the formation of β-sheet-enriched, hydrophobic-patch-containing intermediates; the final result was a lack of aggregation and, in some cases, an inhibition of the spontaneous aggregation of β peptides (figs 3, 4). Consistently

accompanying this, fibril formation was also prevented (fig. 5D). These findings are consistent with other studies also reporting that Cu^{2+}, which appears to boost amyloid aggregation at slightly acidic conditions, is inefficient in or actually prevents the fibrillogenesis process at pH > 7 [22, 24, 52].

The various effects reported in the present paper clearly reflect different metal-peptide interaction modalities. Scientific data based on chemical modification studies suggest that Aβ possesses preferential Zn^{2+}-binding sites in its N-terminal 1–16 domain. The metal ion is postulated to interact with the N_τ atoms of the imidazol ring of His-6, -13 and -14 both at acidic and alkaline pH and the subsequent peptide aggregation occurs through intermolecular His(N_τ)-Zn(II)-His(N_τ) bridges [20, 53]. This Zn^{2+} ligation mode induces an increase in the Tyr-10 fluorescence (fig. 1), which probably reflects a conformational rearrangement of the peptide that brings the fluorophore into a more hydrophobic environment [37] and removes it from the neighborhood of some quenching groups.

At neutral pH, Cu^{2+} has been postulated to preferentially bind to deprotonated amide nitrogens of the peptide main chain and to the N_π atom of the histidine imidazol ring of the N-terminal sequence. This chelation mode leads to a partial destruction of the precursor β sheet structure (see table 1; [53]), thus preventing the formation of intermolecularly cross-linked aggregates.

Much less is known about the preferential regions of aluminum binding to amyloids. Work is in progress in our laboratories to learn more about this crucial point and the data obtained will be the matter of a future communication. On the basis of studies on 'model tangle' sequences, Al^{3+} binds to -COO^- of Glu and Asp and to -OH of Ser and Tyr residues [54]. Binding to Tyr could *per se* explain the fluorescence quenching induced by this ion (fig. 1) since the tyrosinate-like form thus created is very poorly fluorescent [55]. Alternatively, Al^{3+}-binding would mask the fluorophore from nearby quenching groups, in contrast to what is observed with Zn^{2+}. The putative Al^{3+}-chelating amino acid residues are present both in the hydrophilic segment (sequence 1–16) and in the hydrophobic core (sequence 20–35) of the peptides, thus suggesting that the Al^{3+}-binding area is less restricted than that for Zn^{2+} and Cu^{2+}, which is confined to the N-terminal sequence.

The region of metal interaction can be a determinant for the different aggregational potencies of the metals under investigation. Binding of Al^{3+} to carboxylate groups both in the hydrophilic 1–16 segment and the molecule interior would better neutralize the electrostatic repulsions which prevent monomer-monomer interactions, thus favoring hydrophobic bonds which enhance the propensity of the peptide for aggregation.

Several studies have proposed that the initial pathophysiology induced by Aβ might involve alterations in membrane structure. Physico-chemical interaction of oligomeric and polymeric species with membrane domains, including changes in fluidity and binding to membrane components, can be a determining factor for triggering the mechanisms of neurotoxicity. Indeed, a defective regulation of the physical properties of biological membranes is known to lead to deleterious consequences for correct cell functioning. Changes in the membrane fluidity, for instance, have been associated with dysfunctions of membrane receptors, ionic channels and transport proteins [46]. There seems to be a well-documented link between the toxicity and the perturbing effects of Aβ peptides at the level of neuronal membranes. Thus, the effects of Aβ on membrane fluidity have been proposed to contribute to the disruption of various cell neuronal functions (e.g., calcium signaling, activity of various enzymes, and lipid transport) [13, 41–44].

The most recent studies on Aβ in relation to AD converge on the hypothesis that the soluble pre-fibrillar oligomeric entities which exhibit higher affinity for the membrane lipid domains might be responsible for the induction of toxicity at the early stages of AD, whereas insoluble polymeric species might act at the late stages of the disease [for a review see ref. 13]. On this basis, we considered whether Al^{3+} could enhance the membrane-perturbing action typical of β-amyloids. We used Aβ in a range of concentrations which correspond to different soluble aggregated forms (see fig. 3). The results obtained with DMPC liposomes as membrane models indicate that the metal-free 1–42 fragment does not noticeably alter the membrane structure in the solid state, as can be deduced from the almost unchanged value of DPH anisotropy and the limited shift in the critical temperature of the lipid phase transition. Increasing Aβ concentrations, however, cause a modest perturbation of the dynamic properties of the fluid state, which reflects an increase in membrane rigidity, in agreement with similar data previously reported on this system [56]. Clearly, the disordered disposition and high mobility of the acyl chains favors the penetration of the peptide into the core of the bilayer. Such membrane structural changes are dramatically enhanced in the presence of the Aβ-Al^{3+} complex, which brings about a general immobilization of the system. This is most likely the consequence of the higher aggregational capacity of Aβ-Al^{3+} at all the concentrations used (see figs 3, 4). Since these effects are already observed at very low complex concentrations, the influence of Al^{3+} on the membrane structural and functional properties could become very important under physiological conditions where Aβ levels in plasma and cerebrospinal fluids are nanomolar [57], i.e., at much lower levels than those generally used for in vitro experiments. Based on the hypothesis that the intracellular toxicity mediated by Aβ soluble oligomers is more harmful than that induced by extracellular fibrillar polymers [13], the high aggregating potential of Al^{3+} and

strong membrane-perturbing effect of the Al^{3+}-Aβ complex should be particularly emphasized.

On the basis of the above considerations, the cell membrane might clearly represent a target, but also an additional obstacle, when designing drugs to be used against AD. For example, metal chelation by DFO has been proposed as a promising therapy to retard the progression of moderate AD [58]. If the formation of Al^{3+}-amyloid is critical to the etiology of AD, then metal chelation with DFO might not be efficient in countering the effect of the membrane-bound complex in the pre-fibrillar state. Indeed, DFO is not able to neutralize, at least in vitro, the perturbing effects of the Al^{3+}-Aβ complex on membranes, most likely because DFO is a hydrophilic molecule that does not easily penetrate the membrane barrier. However, DFO is very efficient in antagonizing the effects of Al^{3+} in solution, even after late Aβ aggregation, which would imply that such a chelation can act as a protective mechanism by preventing or reverting Aβ aggregation in the extracellular spaces.

Acknowledgments. This project was partially supported by grant CNR/MIUR 449/97-DM 30/10/2000.

1 Munoz D. G. and Feldman H. (2000) Causes of Alzheimer's disease. Can. Med. Assoc. J. **162:** 65–72
2 Hardy J. and Selkoe D. J. (2002) The amyloid hypothesis of Alzheimer's disease: progress and problems on the road to therapeutics. Science **297:** 353–356
3 Pike C. J., Burdick D., Walencewicz A. J., Glabe C. G. and Cotman C. W. (1993) Neurodegeneration induced by beta-amyloid peptides in vitro: the role of peptide assembly state. J. Neurosci. **13:** 1676–1687
4 Harper J. D., Wong S. S., Lieber C. M. and Lansbury P. T. Jr (1999) Assembly of Abeta amyloid protofibrils: an in vitro model for a possible early event in Alzheimer's disease. Biochemistry **38:** 8972–8980
5 Lambert M. P., Barlow A. K., Chromy B. A., Edwards C., Freed R., Liosatos M. et al. (1998) Diffusible, nonfibrillar ligands derived from Abeta 1–42 are potent central nervous system neurotoxins. Proc. Natl. Acad. Sci. USA **95:** 6448–6453
6 Klein W. L., Krafft G. A. and Finch C. E. (2001) Targeting small Abeta oligomers: the solution to an Alzheimer's disease conundrum? Trends Neurosci. **24:** 219–224
7 Walsh D. M., Klyubin I., Fadeeva J. V., Cullen W. K., Anwyl R., Wolfe M. S. et al. (2002) Naturally secreted oligomers of amyloid beta protein potently inhibit hippocampal long-term potentiation in vivo. Nature **416:** 535–539
8 Kayed R., Head E., Thompson J. L., McIntire T. M., Milton S. C., Cotman C. W. et al. (2003) Common structure of soluble amyloid oligomers implies common mechanism of pathogenesis. Science **300:** 486–489
9 Hartley D. M., Walsh D. M., Ye C. P., Diehl T., Vasquez S., Vassilev P. M. et al. (1999) Protofibrillar intermediates of amyloid beta-protein induce acute electrophysiological changes and progressive neurotoxicity in cortical neurons. J. Neurosci. **19:** 8876–8884
10 Howlett D. R., Perr A. E., Godfrey F., Swatton J. E., Jennings K. H., Spitzfaden C. et al. (1999) Inhibition of fibril formation in beta-amyloid peptide by a novel series of benzofurans. Biochem. J. **340:** 283–289
11 Ward R. V., Jennings K. H., Jepras R., Neville W., Owen D. E., Hawkins J. et al. (2000) Fractionation and characterization of oligomeric, protofibrillar and fibrillar forms of beta-amyloid peptide. Biochem. J. **348:** 137–144
12 Walsh D. M., Tseng B. P., Rydel R. E., Podlisny M. B. and Selkoe D. J. (2000) The oligomerization of amyloid beta-protein begins intracellularly in cells derived from human brain. Biochemistry **39:** 10831–10839
13 Talaga P. and Queré L. (2002) The plasma membrane: a target and hurdle for the development of anti-Abeta drugs? Curr. Drug Target CNS Neurol. Disord. **1:** 567–574
14 McLaurin J., Yang D., Yip C. M. and Fraser P. E. (2000) Review: modulating factors in amyloid-beta fibril formation. J. Struct. Biol. **130:** 259–270
15 Bush A. I. (2003) The metallobiology of Alzheimer's disease. Trends Neurosci. **26:** 207–214
16 Exley C. and Korchzhkina O. V. (2001) The association of aluminium and β amyloids in Alzheimer's disease. In: Aluminium and Alzheimer's Disease**:** The Science that Describes the Link, pp. 421–434, Exley C. (ed), Elsevier, Amsterdam
17 Favarato M., Zanoni S., Nicolini M. and Zatta P. (1994) Histofluorimetric aluminum determination in the core of senile plaques from Alzheimer's disease. Life Chem. Rep. 11**:** 71–78
18 Beauchemin D. and Kisilevsky R. (1998) A method based on ICP-MS for the analysis of Alzheimer's amyloid plaques. Anal. Chem. **70:** 1026–1029
19 Lovell M. A., Robertson J. D., Teesdale W. J., Campbell J. L. and Markesbery W. R. (1998) Copper, iron and zinc in Alzheimer's disease senile plaques. J. Neurol. Sci. **158:** 47–52
20 Dong J., Atwood C. S., Anderson V. E., Siedlak S. L., Smith M. A., Perry G. et al. (2003) Metal binding and oxidation of amyloid-b within isolated senile plaque cores: raman microscopic evidence. Biochemistry **42:** 2768–2773
21 Mantyh P. W., Ghilardi J. R., Rogers S., DeMaster E., Allen C. J., Stimson E. R. et al. (1993) Aluminum, iron, and zinc ions promote aggregation of physiological concentrations of beta-amyloid peptide. J. Neurochem. **61:**1171–1174
22 Atwood C. S., Moir R. D., Huang X., Scarpa R. C., Bacarra N. M., Romano D. M. et al. (1998) Dramatic aggregation of Alzheimer A beta by Cu(II) is induced by conditions representing physiological acidosis. J. Biol. Chem. **273:** 12817–12826
23 Atwood C. S., Huang X., Moir R. D., Tanzi R. E. and Bush A. I. (1999) Role of free radicals and metal ions in the pathogenesis of Alzheimer's disease. Met. Ions Biol. Syst. **36:** 309–364
24 House E., Collingwod J., Khan A., Korchazkina O., Berthon G. and Exley C. (2004). Aluminium, iron, zinc and copper influence the in vitro formation of Aβ_{42} in a manner which may have consequences for metal chelation therapy in Alzheimer disease. J. Alzheimer's Dis. **6:** 291–301
25 Zatta P., Favarato M. and Nicolini M. (1993) Deposition of aluminum in brain tissues of rats exposed to inhalation of aluminum acetylacetonate. Neuroreport **4:** 1119–112
26 Bala Gupta V., Anitha S., Hedge M. L., Zecca L., Garruto M. R., Ravid R. et al. (2005) Aluminium in Alzheimer's disease: are we still at a crossroad? Cell Mol. Life Sci. **62:** 143–158
27 Meiri H., Banin E., Roll M. and Rousseau A. (1993) Toxic effects of aluminum on nerve cells and synaptic transmission. Prog. Neurobiol. **40:** 89–121
28 Good P. F. and Perl D. P. (1993) Aluminium in Alzheimer's? Nature **362:** 418–422
29 Kawahara M., Muramoto K., Kobayashi K., Mori H. and Kuroda Y. (1994) Aluminum promotes the aggregation of Alzheimer's amyloid beta-protein in vitro. Biochem. Biophys. Res. Commun. **198:** 531–535
30 Kawahara M., Kato M. and Kuroda Y. (2001) Effects of aluminum on the neurotoxicity of primary cultured neurons and on the aggregation of beta-amyloid protein. Brain Res. Bull. **55:** 211–217
31 Exley C., Price N. C., Kelly S. M. and Birchall J. D. (1993) An interaction of beta-amyloid with aluminium in vitro. FEBS Lett. **324:** 293–295

32 Evans P. and Harrington C. (1998) Aluminosilicate particulate and beta-amyloid in vitro interactions: a model of Alzheimer plaque formation. Biochem. Soc. Trans. **26:** S251

33 Practicò D., Urhyu K., Sung S., Tang S., Trojanowski J. Q. and Lee V. M. (2002) Aluminum modulates brain amyloidosis through oxidative stress in APP transgenic mice. FASEB J. **16:** 1138–1140

34 Zatta P., Zambenedetti P., Bruna V. and Filippi B. (1994) Activation of acetylcholinesterase by aluminum (III): the relevance of the metal species. Neuroreport **5:** 1777–1780

35 Bohm G., Muhr R. and Jaenicke R. (1992) Quantitative analysis of protein far UV circular dichroism spectra by neural networks. Protein Eng. **5:** 191–195

36 Kremer J. M., Esker M. W., Pathmamanoharan C. and Wiersema P. H. (1977) Vesicles of variable diameter prepared by a modified injection method. Biochemistry **16:** 3932–3935

37 Garzon-Rodriguez W.,Yatsimirsky A. K. and Glabe C. G. (1999) Binding of Zn(II), Cu(II) and Fe(III) ions to Alzheimer's Aβ peptide studied by fluorescence. Bioorg. Med. Chem. Lett. **9:** 2243–2248

38 Kasha M. (1952) Collisional perturbation of spin-orbital coupling and the mechanism of fluorescence quenching: a visual demonstration of the perturbation. J. Chem. Phys. **20:** 71–74

39 Uversky V. N., Lee H. J., Li J., Fink A. L. and Lee S. J. (2001) Stabilization of partially folded conformation during alpha-synuclein oligomerization in both purified and cytosolic preparations. J. Biol. Chem. **276:** 43495–43498

40 LeVine H. (1993) Thioflavine T interaction with synthetic Alzheimer's disease beta-amyloid peptides: detection of amyloid aggregation in solution. Protein Sci. **2:** 404–410

41 Arispe N., Rojas E. and Pollard H. B. (1993) Alzheimer's disease amyloid beta protein forms calcium channels in bilayer membranes: blockade by tromethamine and aluminium. Proc. Natl. Acad. Sci. USA **90:** 567–571

42 Hartmann H., Eckert A. and Muller W. E. (1994) Characterization of the interactions of Alzheimer beta-amyloid peptides with phospholipid membranes. Biochem. Biophys. Res. Commun. **200:** 1185–1192

43 McLaurin J. and Chakrabartty A. (1997) Characterization of the interactions of Alzheimer beta-amyloid peptides with phospholipid membranes. Eur. J. Biochem. **245:** 355–363

44 Lin H., Bhatia R. and Lal R. (2001) Amyloid beta protein forms ion channels: implications for Alzheimer's disease pathophysiology. FASEB J. **15:** 2433–2444

45 Zatta P., Ibn-Lkhayat-Idrissi M., Zambenedetti P., Kilyen M. and Kiss T. (2002) In vivo and in vitro effects of aluminum on the activity of mouse brain acetylcholinesterase. Brain Res. Bull. **59:** 41–45

46 Szöllosi J. (1994) Fluidity/viscosity of biological membranes. In: Mobility and Proximity in Biological Membranes, pp 137–208, Damianovich S., Edidin M., Tron L. and Szöllosi J. (eds), CRC Press, Boca Raton

47 Kruck T. P. A. and Burrow T. E. (2002) Synthesis of Feralex, a novel aluminium/iron chelating compound. J. Inorg. Biochem. **88:** 9–24

48 Cuajungco M. P., Faget K. Y., Huang R. E., Tanzi R. E. and Bush A. I. (2000) Metal chelation as a potential therapy for Alzheimer's disease. Ann. N. Y. Acad. Sci. **920:** 293–304

49 Di Vaira M., Bazzicalupi C., Orioli PL., Messori L., Bruni B. and Zatta P. (2004) Clioquinol, a drug for Alzheimer's disease specifically interfering with brain metal metabolism: structural characterization of its zinc(II) and copper(II) complexes. Inorg. Chem. **43:** 3795–3797

50 Kopito R. R. (2000) Aggresomes, inclusion bodies and protein aggregation. Trends Cell Biol. **10:** 524–530

51 Zatta P. and Alfrey A.C. (eds) (1995) Aluminum Toxicity in Infants' Health and Disease, Wold Sci, Singapore

52 Bush A. I. and Tanzi R. E. (2002) The galvanization of β-amyloid in Alzheimer's disease. Proc. Natl. Acad. Sci. USA **99:** 7317–
7319

53 Miura T., Suzuki K., Kohata N. and Takeuchi H. (2000) Metal binding modes of Alzheimer's amyloid beta-peptide in insoluble aggregates and soluble complexes. Biochemistry **39:** 7024–7031

54 Fasman G. D. (1996) Aluminum and Alzheimer's disease: model studies. Coord. Chem. Rev. **149:** 125–165

55 Lakowicz J. R. (1983) Principles of Fluorescence Spectroscopy, Plenum, New York

56 Kremer J. J., Sklansky D. J. and Murphy R. M. (2001) Profile of changes in lipid bilayer structure caused by beta-amyloid peptide. Biochemistry **40:** 8563–8571

57 Tamaoka A., Sawamura N., Fukushima T., Shoji, S., Matsubara E., Shoji M. et al. (1997) Amyloid beta protein 42(43) in cerebrospinal fluid of patients with Alzheimer's disease. J. Neurol. Sci. **148:** 41–45

58 Crapper McLachlan D. R., Dalton A. J., Kruck T. P., Bell M. Y., Smith W. L., Kalow W. et al. (1991) Intramuscular desferrioxamine in patients with Alzheimer's disease. Lancet **337:** 1304–1308